Kinesin and Dynein-Dynactin at Intersecting Microtubules: Motor Density Affects Dynein Function

Jennifer L. Ross, Henry Shuman, Erika L. F. Holzbaur, and Yale E. Goldman
Pennsylvania Muscle Institute and Department of Physiology, University of Pennsylvania, Philadelphia, Pennsylvania

ABSTRACT Kinesin and cytoplasmic dynein are microtubule-based motor proteins that actively transport material throughout the cell. Microtubules can intersect at a variety of angles both near the nucleus and at the cell periphery, and the behavior of molecular motors at these intersections has implications for long-range transport efficiency and accuracy. To test motor function at microtubule intersections, crossovers were arranged in vitro using flow to orient successive layers of filaments. Single kinesin and cytoplasmic dynein-dynactin molecules fused with green-fluorescent protein, and artificial bead cargos decorated with multiple motors, were observed while they encountered intersections. Single kinesins tend to cross intersecting microtubules, whereas single dynein-dynactins have a more varied response. For bead cargos, kinesin motion is independent of motor number. Dynein beads with high motor numbers pause, but their actions become more varied as the motor number decreases. These results suggest that regulating the number of active dynein molecules could change a motile cargo into one that is anchored at an intersection, consistent with dynein's proposed transport and tethering functions in the cell.

INTRODUCTION

Kinesin-1 and cytoplasmic dynein are the major cytoplasmic motors responsible for long-range transport in many cell types. Kinesin walks along microtubules toward the plus ends, facilitating material transport from the cell interior toward the cortex. Dynein transports material toward the microtubule minus ends, moving from the cell periphery to the cell interior.

Although both proteins are microtubule-based transport motors, they are structurally distinct. Conventional kinesin is primarily a homodimer of heavy chains that each fold into a compact motor head ~4 nm in diameter. Crystal structures show that ATP hydrolysis at a single catalytic site causes conformational changes in the head (1). These structural changes alter the motor head's affinity for the microtubule and lead to nanometer-scale motions of a short linker region that extends from the globular head. The C-terminus of kinesin heavy chain is a dimerization domain that mediates the assembly of the two-headed motor. Alternating and coordinated ATP hydrolysis at each of the two heads causes the kinesin to step processively and robustly along the microtubule (2). Kinesin's C-terminal tail can bind to cargo directly or via two light chains that have been implicated in regulation of kinesin by autoinhibition (1,3).

Dynein is also composed primarily of a dimer of heavy chains. These polypeptide chains are considerably longer and fold to form motor domains that are much larger (10 nm) than those of kinesin (1). There are multiple sites for ATP binding and, potentially, hydrolysis within each head domain (4). The most critical catalytic site is 15–20 nm away from the microtubule-binding site, which is at the end of a protruding stalk (5,6). The two motor domains are each connected to a long, flexible tail. These tail domains mediate dimerization as well as association with additional intermediate and light chains. Although the two heads do not appear to be tightly coupled, dynein has been shown to exhibit processive stepping (7–11). Dynein motility is further enhanced by the dynein-activating complex dynactin, which binds directly to the dynein intermediate chain (7,12,13).

These structural distinctions result in significant differences between the two motors in biophysical assays. In particular, kinesin has been shown to walk along a single protofilament of the microtubule, taking 8-nm steps (2,14). Dynein, on the other hand, wanders across the microtubule surface with steps that vary from 8 to 32 nm (8,9,11), including runs in the reverse (plus-end) direction (10).

Although assays with motors on single microtubules reveal many intrinsic features and capabilities of the motor proteins, the cellular environment is much more complex than the simple geometry contrived in vitro. In vivo, intersections among the microtubules, actin, and intermediate filaments have been shown to affect transport within the cell (15–17). Cytoskeletal microtubules primarily form a polarized radial network, but they are found to intersect at a variety of angles both near the nucleus and at the cell periphery, areas known for cargo sorting (18,19). The behavior of kinesin and dynein at microtubule intersections has implications for transport efficiency and accuracy because intersecting microtubules serve both as switching points for direction alteration and also as potential obstacles to motion. The impact of such complex microtubule configurations on motor protein function is not known. To study the response of motor

Submitted August 17, 2007, and accepted for publication October 18, 2007.

Address reprint requests to Yale E. Goldman, Pennsylvania Muscle Institute and Dept. of Physiology, 3700 Hamilton Walk, University of Pennsylvania, Philadelphia, PA 19104. E-mail: goldmany@mail.med.upenn.edu.

Jennifer L. Ross's present address is Dept. of Physics, University of Massachusetts, Amherst, MA.

Editor: Susan P. Gilbert.

0006-3495/08/04/3115/11 $2.00

doi: 10.1529/biophysj.107.120014

proteins at microtubule intersections and to model a common aspect of the in vivo situation, we have taken the approach of building an element of complexity into in vitro systems by examining single-motor dynamics in a system of intersecting microtubules.

We assembled microtubule crossovers in vitro by successively adding microtubules into a flow chamber in orthogonal directions. Single fluorescently labeled motors, or bead cargos decorated with multiple motors, were observed to travel along microtubules and interact with crossing microtubules. We found that dynein navigates well at low motor concentrations but tethers cargo at crossovers at high motor density. This behavior suggests that dynein can function in the cell both as a cargo transporter and as a cargo anchor, depending on motor number. Kinesin, on the other hand, negotiates past intersections at all concentrations. In addition, kinesin can deform the microtubule tracks, which could contribute to microtubule network rearrangements in vivo. These varied responses are most likely explained by dynein's flexible structure in comparison to kinesin and are indicative of the different functions of these motors in the cell.

MATERIALS AND METHODS

Crossed microtubules in vitro

Flow chambers were assembled from two coverslips bound at the corners by double-stick tape to make two perpendicular crossed flow paths (Fig. 1 *A*). To bind the microtubules to the coverslips, a biotin-streptavidin system was employed. First, 10 μl of biotinylated-BSA solution (1 mg/ml, Sigma, St. Louis, MO) was flowed in to coat the coverglasses, incubated for 2 min, and washed out with three chamber volumes of wash buffer (5 mg/ml BSA, 20 μM Taxol (Cytoskeleton, Denver, CO), 10 mM DTT in motility assay buffer (MAB; 50 mM potassium acetate, 10 mM Na-PIPES, 5 mM $MgSO_4$, 1 mM EGTA)). Second, 10 μl of streptavidin solution (2 mg/ml streptavidin (Sigma) in wash buffer) was flowed in, incubated for 2 min, and washed out with three chamber volumes of wash buffer. Third, 10 μl of biotinylated, rhodamine-labeled microtubules (1:50 biotin-tubulin (Cytoskeleton), 1:50 rhodamine-tubulin (Cytoskeleton), final concentration 0.45 μM tubulin, 20 μM Taxol in MAB) were flowed into the chamber in the direction of the *y* axis (Fig. 1 *A*), allowed to incubate for 30 s, and washed out with wash buffer. Fourth, 10 μl of biotinylated, rhodamine-labeled microtubules were flowed into the chamber in the direction of the *x* axis (Fig. 1 *A*), allowed to incubate for 30 s, and washed out with wash buffer. The result is that microtubules flowed along the *y* axis are bound closer to the coverslip, and we refer to them as ''underpass'' microtubules. The microtubules flowed along the *x* axis are held away from the coverslip at crossovers; they are termed ''overpass'' microtubules (Fig. 1, *B* and *C*).

Kinesin constructs and purification

A truncated human kinesin heavy chain construct (560 amino acids) was expressed in bacteria and purified using the 6×-His tag (20). Further purification via a sucrose density gradient was used to eliminate His-tagged fragments that could bind to beads, as previously described (21). Constructs for GFP-kinesin and 6×-His-tagged kinesin were a gift from R. Vale (UCSF). Purity was assessed by Coomassie blue staining of SDS-PAGE gels after purification, and concentrations of useable fractions were determined to be 30 μg/ml by comparison to a BSA dilution series run on the same gel (see Supplementary Material, Fig. S3 *A*). Motility was assessed using filament-gliding assays, single-molecule fluorescence assays, and bead assays. At 1 mM MgATP, single-molecule velocity was 560 ± 30 nm/s for GFP-kinesin, which is typical for this construct (22).

Dynein-dynactin purification

Dynein-dynactin complexes were purified from mouse or bovine brain tissue using sucrose gradient separation as previously described (10,12). GFP-labeled dynein-dynactin complexes were purified from transgenic mice expressing a GFP-labeled dynactin subunit, the same line as described previously

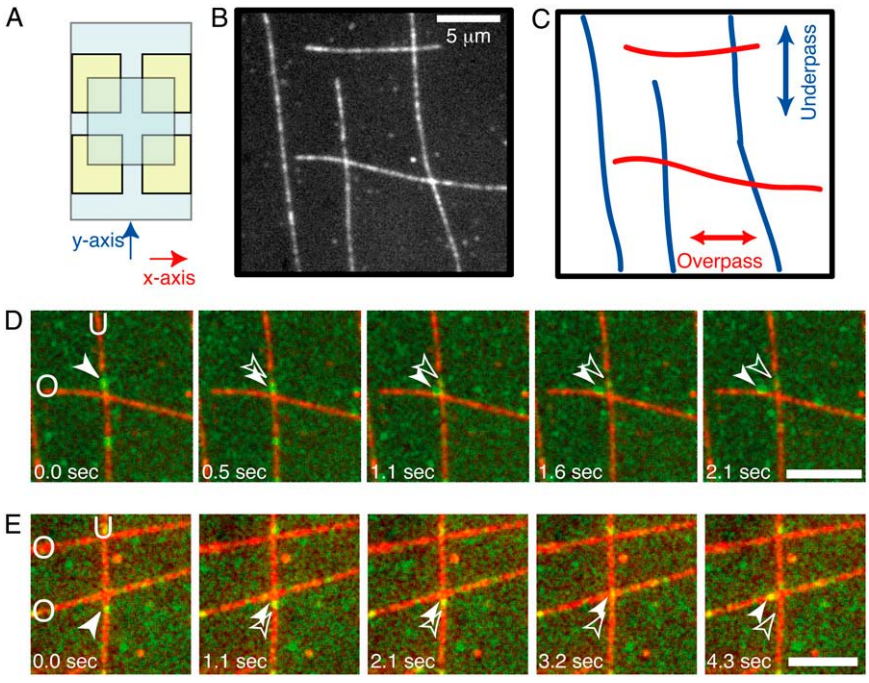

FIGURE 1 Experimental crossed-flow-path sample chamber and resulting microtubule array. (*A*) Schematic of crossed-flow-path chamber. The bottom coverglass is 22 mm × 40 mm (*pale blue*). Four square pieces of double-sided adhesive tape (*yellow*) are arranged to make two perpendicular 3-mm-wide flow paths. The top coverglass is 18 mm × 18 mm. We denote the flow paths as the *x*- and *y*-directions. (*B*) Example image of rhodamine- and biotin-labeled microtubules bound to the coverglass of a crossed-path flow chamber. Scale bar: 5 μm. (*C*) Schematic of the same location in *B* to highlight the crossing microtubule tracks. (*D*) A single GFP-kinesin, imaged using total internal reflection microscopy, starts walking on the vertical, underpass microtubule (U) and switches to walking on the horizontal, overpass (O) microtubule. (*E*) A single dynein-dynactin-GFP complex, imaged using total internal reflection fluorescence microscopy, starts walking on the vertical, underpass microtubule (U) and switches to walking on the horizontal, overpass microtubule (O). Green image is GFP fluorescence. Red image is rhodamine fluorescence. Scale bars: 5 μm. See supplementary movies and Fig. S1 for raw images without false coloring.

(10). Purity and integrity of the dynein-dynactin complex was assessed by Coomassie blue staining of SDS-PAGE gels and Western blotting for dynein and dynactin subunits after purification. The concentration of dynein heavy chain was determined to be 18 μg/ml by SDS-PAGE gel and Coomassie blue staining and comparison with a BSA dilution series on the same gel (see Fig. S3 *B*). Motility was assessed using filament-gliding assays, single-molecule fluorescence assays, and bead assays. At 1 mM MgATP, single complexes of dynein-dynactin-GFP exhibited velocities of 980 $\pm$ 70 nm/s, which is typical for this preparation (10).

Single-molecule total internal reflection fluorescence microscopy assays

Purified GFP-labeled kinesin or dynein-dynactin complexes in MAB with Taxol (20 μM), ATP (1 mM, Sigma), glucose oxidase (1 μg/ml, Sigma), catalase (940 units/mg, Sigma), and glucose (30 mg/ml) were flowed into the crossed-flow chamber and observed via total internal reflection fluorescence (TIRF) microscopy. Total internal reflection excitation was generated on an inverted microscope by projecting 488-nm light from an argon ion laser through a top-mounted 60×, 1.45 NA condenser objective lens (Olympus, Center Valley, PA). Image sequences were collected using an electron multiplier CCD camera (Andor, South Winsor, CT). An image of the microtubules was recorded in epifluorescence at the beginning of the image sequence to determine the location of the microtubule intersections. The maximum fluorescence intensity was assumed to be the middle of the microtubule and was used as the microtubule location. Data were viewed and scored by overlaying a representation of the microtubule intersection onto the single-molecule movement movie in ImageJ (NIH, Bethesda, MD). Accuracy of localization by this method was ~300 nm because of the point-spread function. When a single motor complex moved by one spot diameter (~300 nm) around the intersection, the motion was scored as a pass, switch, or reverse. If the molecule stayed at the intersection for more than one frame, it was scored as a pause. If a molecule disappeared, it was scored as dissociation. Further analysis using two-dimensional Gaussian fitting and particle tracking was performed on motor complexes that were bright and well separated from nearby fluorophores using a plug-in specifically written in our laboratory for ImageJ (10). Two-dimensional Gaussian analysis had an accuracy of 25 nm and revealed the same statistics as scoring.

The rate of photobleaching by the TIRF illumination was determined using GFP-labeled dynein and kinesin bound nonspecifically to the coverglass surface. The GFP fluorescence for kinesin lasted ~100 s, and that for dynein-dynactin lasted 250 s. These times were approximately 10 times longer than the association time of the GFP-labeled motors translocating along microtubules. This result indicates that, in the main experiments, most instances of disappearance of the GFP fluorescence were the result of dissociation of the motor from the microtubule rather than photobleaching of the fluorophore.

Multiple motors on artificial bead cargo assays

For kinesin bead assays, streptavidin-conjugated, 0.8-μm-diameter beads (Spherotech, Lake Forest, IL) were incubated with biotinylated antibody to penta-His and stored at 4°C for up to 1 month (23). Beads were sonicated for 2 min before being added to kinesin. Beads (2 μl) plus diluted kinesin (2 μl of 0.001, 0.002, 0.005, 0.01, 0.02, or 0.04 dilutions of the 30 μg/ml stock) were incubated for 1 h on ice to bind motors. An additional 16 μl of wash buffer with Taxol (20 μM), ATP (1.25 mM), *d*-biotin (1 mg/ml, Sigma), glucose oxidase (0.5 μg/ml), catalase (470 units/ml), and glucose (15 mg/ml) was added before introduction into the chamber.

For dynein-dynactin bead assays, 1-μm polystyrene beads (Polysciences, Warrington, PA) were diluted 100-fold to make a working solution. Beads (6 μl) plus diluted dynein-dynactin (6 μl of 0.05, 0.1, 0.2, or 1 dilutions of the 17 μg/ml stock) were incubated for 2 min on ice, when wash buffer with casein (5 mg/ml) was added to halt binding (8). An additional 6 μl wash buffer with Taxol (20 μM), ATP (3.3 mM), glucose oxidase (0.5 μg/ml), catalase (470 units/ml), and glucose (15 mg/ml) was added before introduction into the chamber.

Motor binding to beads was assessed by Western blots of the supernatants and pellets after centrifugation of the beads, including a standard of known motor concentration (antibodies used were kinesin heavy-chain antibody 1614 (Chemicon, Billerica, MA) and dynein intermediate-chain antibody 1618 (Chemicon)). We found that the protein left in the supernatant was below detectable levels, which were ~1 nM for dynein intermediate chain (7% of the maximum dilution used) and 1 nM for kinesin heavy chain (8% of the maximum dilution used), indicating that essentially all of the motors in the mixtures bound to beads, as expected (data not shown).

Motor-decorated beads were flowed into the crossed-path flow chamber. An optical trap was used to place beads on microtubules near intersections. Image sequences were collected using the Andor Ixon camera. An image of the microtubules was recorded in epifluorescence at intervals throughout the image sequence to determine the location of the bead with respect to the microtubule intersections.

For kinesin-decorated beads, the optical trap was used to measure the stall force at two different kinesin concentrations (0.001 and 0.02) (Fig. S4). Beads with 0.001 relative kinesin concentration were in the single-motor range with an average stall force of 4.2 pN, which is typical for recombinant kinesin (24). The optical trap setup was similar to that described by Takagi et al. (25) with the modification that only one trap was used.

RESULTS

Microtubule intersections were made by flowing biotinylated microtubules into a flow chamber with two perpendicular flow paths (Fig. 1 *A*, see Experimental Procedures). Microtubules were flowed first in one direction and then in the perpendicular direction, resulting in orthogonally crossed microtubules bound to the coverglass (Fig. 1 *B*). Those microtubules that are aligned with the first flow direction are closer to the glass surface at the intersection and are termed ''underpass'' microtubules (Fig. 1 *C*, *blue*). Those microtubules that are aligned in the perpendicular flow direction are further away from the glass surface at the intersection and are called ''overpass'' microtubules (Fig. 1 *C*, *red*).

Single motor complexes at intersections

GFP-labeled motor complexes of kinesin or dynein-dynactin were added to the flow chamber. These motor complexes were well-characterized in previous single motor assays on individual microtubules (10,22). Individual GFP-motor complexes were imaged and recorded at 2 frames/s using TIRF microscopy as they moved along microtubules near intersections. Velocities of single motors were as expected for kinesin (560 $\pm$ 30 nm/s) and dynein-dynactin (980 $\pm$ 70 nm/s) at 1 mM MgATP on nonintersecting microtubules.

On encountering an intersection, motors can exhibit different actions: to pass the intersection on the same microtubule, to pause at the intersection, to switch to the perpendicular microtubule, or to dissociate. Dynein-dynactin can also reverse direction because this motor can make long movements (>300 nm) toward the plus end of microtubules under conditions of low load (10). An epifluorescence image of the microtubules was used to determine the locations of the intersections, and

specific criteria were used to score the actions of individual motor complexes. When a motor reached an intersection, the encounter was scored as a pass event if the motor moved at least 300 nm beyond the intersection while continuing along the original microtubule. A pause event was counted if a motor spent at least 3 frames (>1 s) located at the intersection. A switching event was scored when the motor moved at least 300 nm away from the intersection on the perpendicular microtubule (see example in Fig. 1, *D* and *E*; raw data supplied in Supplementary Material, Fig. S1, *A* and *B*). A reversal event was counted when the motor retraced its path along the same microtubule for at least 300 nm after approaching an intersection. A dissociation event was tallied when the GFP signal disappeared from view at the intersection. A molecule could also disappear if the fluorophore photobleached, but in the present conditions, the rate of bleaching was ~10-fold lower than the rate of dissociation during normal motility (see Experimental Procedures). Thus, most molecules (90%) dissociated when the GFP signal was lost. Fig. 1 shows examples of an individual kinesin (panel *D*) and an individual dynein-dynactin motor complex (panel *E*) switching from one microtubule to an intersecting microtubule.

Of 164 encounters of single GFP-kinesins with microtubule intersections, where approximately half were on overpass microtubules ($n = 85$) and the rest were on underpass microtubules, the majority of encounters resulted in passing or dissociation events (Fig. 2 *A* and Supplementary Material, Table S1). On an overpass, kinesin was most likely to pass, but frequently dissociated (Fig. 2 *A*, *light red bars*). Not surprisingly, kinesin motors were less likely to pass the intersection traveling on an underpass, with a corresponding increase in dissociation events (Fig. 2 *A*, *dark red bars*). Kinesin motors dissociated twice as often from the underpass microtubule as from the overpass (32% and 16%, respectively) most likely because the overpass microtubule acts as an obstacle to motion (Fig. 2 *A*). These differences in passing and dissociating on an overpass versus an underpass were statistically significant (Student's *t*-test, $p < 0.05$). Only a small fraction of kinesin motors switched or paused at the intersection, with approximately the same likelihood from overpass and underpass microtubules (Fig. 2 *A*).

For 154 encounters of single dynein-dynactin-GFP complexes with microtubule intersections, of which 88 were on overpass microtubules and the rest were on underpass microtubules, dynein displayed a more varied response to encountering the microtubule intersection. Dynein showed a significant amount of passing, pausing, switching, dissociating, and reversing on both overpass and underpass microtubules (Fig. 2 *B* and Table S1). On an overpass, the motor complexes were most likely to pass the intersection or switch microtubule tracks, but a significant fraction paused, dissociated, or reversed direction (Fig. 2 *B*, *light blue*). The trend was similar on the underpass microtubules (Fig. 2 *B*, *dark blue*). For dynein, there were no statistically significant differences between motors on overpass versus underpass microtubules.

To determine whether the relative positions of the two microtubules were similar at different intersections, multiple motors were observed to interact at each intersection. For the most part, results at an individual intersection displayed similar statistics to those in the whole data set, implying that the relative positions of underpass and overpasss microtubules were similar and probably touching.

Bead cargos with multiple motors at intersections

In order to model the actions of intracellular cargos such as organelles at microtubule intersections, we introduced polystyrene beads coated with motors at various concentrations into the flow chambers with crossed microtubules. An optical trap was used to place beads on microtubules near intersections. Encounters of beads with microtubule intersections were recorded in bright-field or fluorescence microscopy at 4 frames/s.

Similar to single motor molecules, bead cargos displayed various actions on encountering an intersection: passing, pausing, switching, dissociation, or reversing. Events were scored as a pass, switch, or reverse if the apparent center of the bead moved more than ~1 μm (one bead diameter) away from the intersection; most beads were observed to move significantly farther. Ambiguous movements (< 3% of total

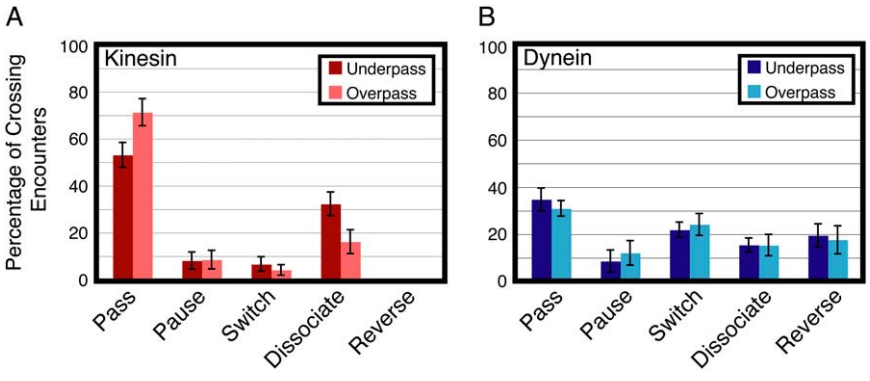

FIGURE 2 Outcomes of GFP-labeled single motor complexes on encountering a microtubule intersection from an overpass or an underpass. (*A*) Actions of single molecules of kinesin-GFP when encountering an intersection from the underpass (*dark red*) or overpass (*light red*) (mean ± SE; $n > 60$). Kinesin motors mostly pass and dissociate at intersections. (*B*) Actions of single molecules of dynein-dynactin-GFP when encountering an intersection from the underpass (*dark blue*) or overpass (*light blue*) (mean ± SE; $n > 30$). For dynein-dynactin, all five actions are about equally likely when a complex approaches from an overpass or underpass microtubule.

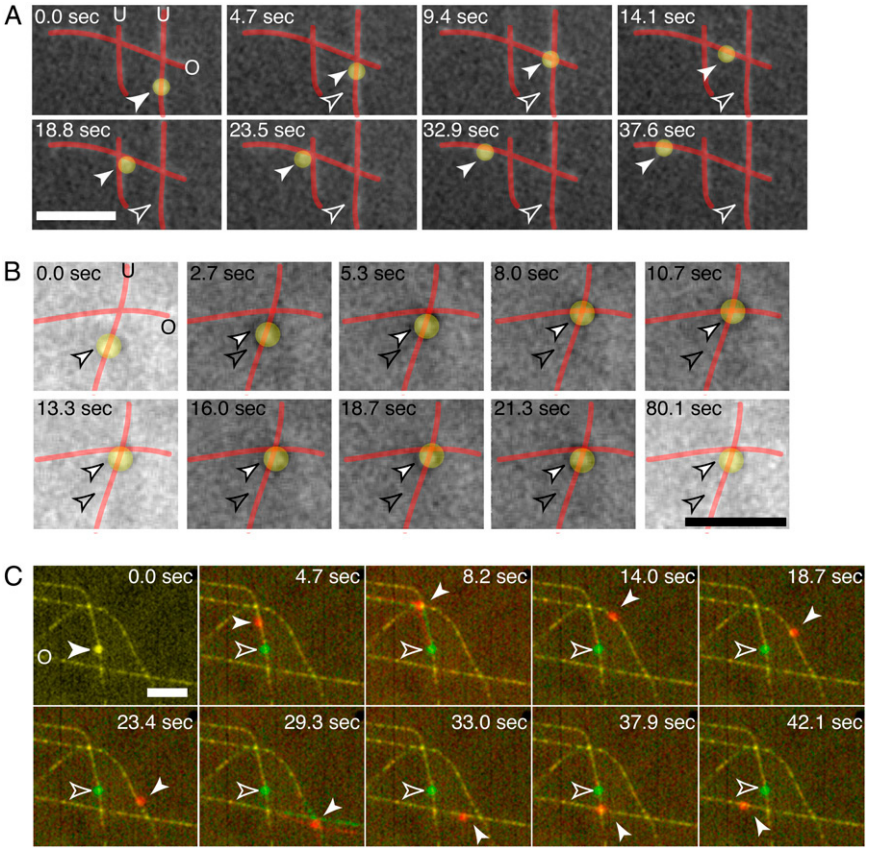

FIGURE 3 Sample time series of motor-decorated bead cargos switching between perpendicular microtubules at an intersection. (*A*) A bead (*false-colored yellow*) is coated with multiple kinesin motors and observed to walk along the microtubules (*red*). The bead is observed to switch from underpass to overpass at the first intersection and then pass by an intersection on an overpass. (*B*) A bead (*false-colored yellow*) is coated with multiple dynein-dynactin complexes and observed to walk along the microtubules (*red*). The bead is observed to pause at an intersection. (*C*) A bead is coated with multiple kinesin motors and observed to switch tracks and pass at various intersections. In the color overlay, the green image shows the positions of the bead and microtubules at the start of the assay (0.0 s), and the red images are the subsequent ones in the time series. At time points 8.2 and 29.3 s, the microtubules are observed to flex and pivot about the intersection as a result of the kinesin-coated bead interacting strongly with both simultaneously. Each image here consists of four images averaged to highlight microtubule bending. Scale bars: 5 μm. For all images, the white, outlined arrow denotes the starting position, and the filled arrow denotes the position at each time point. The underpass microtubules are marked with a ''U'', and the overpass microtubules are marked with an ''O'' in the first frame. See supplementary movies and Fig. S2 for raw images without false coloring.

events) were not scored. Examples of beads decorated with kinesin or dynein-dynactin are shown in Fig. 3, *A* and *B*, respectively; raw images supplied in Fig. S2, *A* and *B*). Dissociation events decreased, and run length increased, as the number of motors on the beads increased for both dynein and kinesin, as expected (data not shown) (26).

Kinesin cargos sometimes flexed or pivoted the microtubules as the bead simultaneously interacted with both microtubules at an intersection. An example is shown in Fig. 3 *C*, at 8.2 and 29.3 s (in the *overlays* the *green images* show the positions of the microtubules at the start of the assay, and the *red images* are the subsequent images in the time series; see Fig. S2 *C* for original images of the same data). Because the microtubules are bound to the glass via biotin-streptavidin, their movement is relatively restricted, and they most often flex from their original positions by $\sim$1 μm, as observed in the example.

Kinesin-decorated bead cargos

Beads coated with kinesin bound to and moved robustly along microtubules at a variety of motor decoration densities. All beads that bound to the microtubules were observed to move actively along the microtubule, indicating that the bound motors were fully functional. The number of beads that bound to microtubules increased with motor density, as previously observed (see Fig. 5 *A*) (27).

At all kinesin concentrations examined, the majority of kinesin beads passed the intersection when traversing on an overpass microtubule; most kinesin beads switched when traversing on an underpass microtubule (Fig. 4 *A* and Table S1). From the bead data and the single-molecule TIRF data (Fig. 4 *A*, *far left*), single molecules usually passed whereas beads most often switched at the intersection ($p < 0.001$, Student's *t*-test). The size of the bead is a definite impediment to beads passing at the intersection. Single molecules may be able to pass under the crossing microtubule, but the bead is too large. Thus, the intersecting microtubule is an obstacle to forward movement, although other motors on the bead can bind to the intersecting microtubule to enable a switch event. Thus, kinesin motors can keep the bead progressing, but on a new microtubule track.

Surprisingly, a small fraction of the cargo can cross through the intersection when starting on an underpass. One possibility is that the bead is able to make two consecutive switches (a double switch) wherein the bead cargo switches from under- to overpass followed immediately by a second switch from over- to underpass. This idea is supported by the fact that beads appeared to interact with both microtubules at these intersections (Fig. 3 *C*). In addition, the overpass microtubule stayed in focus as the bead passed, implying that the bead went over the intersection, not under it. From our data, the probability of passing from an underpass is 17%, which is very close to that expected from the product of each indi-

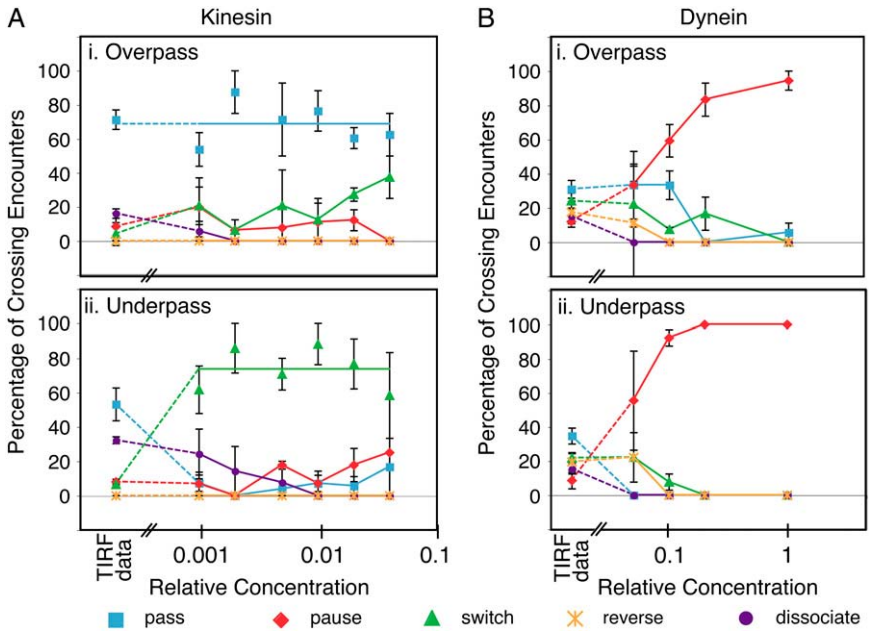

FIGURE 4 Interactions of kinesin- and dynein-dynactin-decorated beads on encountering intersections plotted versus relative density of motors bound to the bead. (*A*) Bead cargos coated with kinesin at a variety of decoration densities showed similar statistics when traversing on the (*i*) overpass or (*ii*) underpass microtubule. In *i* the blue line indicates the average percentage of single molecules and beads passing for all kinesin densities. In *ii*, the green line indicates the average percentage of beads switching for all kinesin densities. (*B*) Bead cargos coated with dynein-dynactin show a large dependence on motor number when traversing on the overpass (*i*) or underpass (*ii*) microtubule. For all plots: passes (*blue squares and lines*), pauses (*red diamonds and lines*), switches (*green triangles and lines*), dissociation (*orange stars and lines*), and reversals (*purple circles and lines*); the leftmost symbols denote the single-molecule TIRF data for comparison. Dashed lines are drawn from the TIRF data to the bead data as a guide to the eye.

vidual switch: probability of switching twice = p(under → over) × p(over → under) = 0.58 × 0.38 = 0.22 (Table S1). Therefore, we conclude that when a bead passes from an underpass, it is the result of a double switch.

The dissociation of kinesin cargos for beads traveling on the underpass microtubule decreased as the motor density increased (Fig. 5 *B*). The data are well fitted by the expression $p_{\text{dissociation}} = p_{\max} \exp(-[\text{Kin}]/R_{\text{k,2U}})$, where $p_{\max} = 34.4\%$, [Kin] is the kinesin concentration relative to the stock concentration, and $R_{\text{k,2U}} = 0.0027$ is a fitting parameter. Interestingly, in the relation describing the probability of a bead binding to the microtubule and actively moving it ($p_{\text{bind}} = 100 \times (1 - \exp(-[\text{Kin}]/R_{\text{k,1}}))$ (Fig. 5 *A*)), the fitting parameter is also $R_{\text{k,1}} = 0.0027$. Single kinesin molecules are processive, so $p_{\text{bind}}/100$ corresponds to the Poisson probability that one or more motors is located on the bead within range of the microtubule on initial placement of the bead by the optical trap. Conversely, $1 - p_{\text{bind}}/100 \exp(-[\text{Kin}]/R_{\text{k,1}})$ is the probability that no motors are located near the microtubule. Essentially the same relation applies to the likelihood that a bead will dissociate at an intersection ($p_{\text{dissociation}} \propto 1 - p_{\text{bind}}/100$ and $R_{\text{k,2U}} = R_{\text{k,1}}$). This result implies that having one or more kinesins located where the bead contacts an overpass microtubule is sufficient to facilitate a switch; conversely, if no motors are within range, the bead will dissociate.

Dynein-dynactin-decorated bead cargos

Dynein-dynactin motor complexes were bound to polystyrene beads at a variety of motor densities. At all motor densities, 95% of dynein-dynactin beads that bound to microtubules were motile. Dynein-coated beads showed considerable displacements in the lateral direction (wobble) as they walked along the microtubules toward the intersections at all motor densities, as previously reported (11). Once bead cargos reached an intersection, their behavior was highly dependent on the number of motors decorating the bead (Fig. 4 *B* and Table S1).

Dynein-dynactin-coated beads paused at all concentrations more often than passing, switching, dissociating, or reversing (Fig. 4 *B* and Table S1). When the beads paused, they remained at the intersection for the duration of observation (up to 10 min). Often, when a new field of view was observed, beads were already accumulated at the intersections. At intermediate dilutions, the percentage of beads that paused depended on which microtubule the bead started traveling; beads on underpass microtubules were more likely to pause than those on overpass microtubules (Fig. 5 *D*).

The percentage of pausing dynein-dynactin beads increased markedly as the density of motors increased on the beads (Fig. 5 *D*). The percentage of pausing beads as a function of relative dynein-dynactin concentration either on underpass or overpass microtubules is fit with the expression $p_{\text{pause}} = 100 \times (1 - \exp(-[\text{Dyn}]/R_{\text{d,2}})$, where [Dyn] denotes the dynein-dynactin concentration relative to the stock concentration. The fitting parameter for the underpass data is $R_{\text{d,2U}} = 0.052$, and for the overpass data is $R_{\text{d,2O}} = 0.114$. Comparing these two values shows that fewer dynein-dynactin complexes are necessary for pausing at the intersection from an underpass than from an overpass. As with kinesin beads, the exponential constants for pausing were similar to the constant for binding of beads, $R_{\text{d,1}} = 0.096$ (Fig. 5 *C*), indicating that one or a few dyneins at the region of a bead that approaches the intersecting microtubule is/are sufficient to tether the bead at the intersection. Presumably, at least one dynein interacting with the original microtubule and one

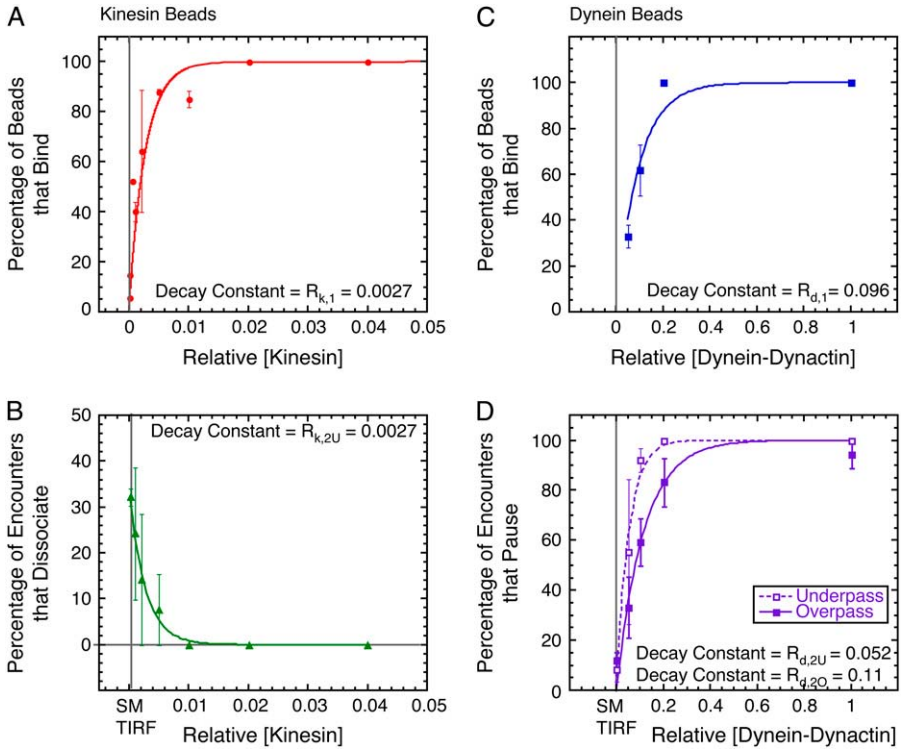

FIGURE 5 Comparison of binding statistics and actions at intersections for kinesin- and dynein-dynactin-coated beads. (*A*) Percentage of kinesin-coated beads that bound microtubules (*red circles*) as a function of relative kinesin concentration and fit to the data (*red line*, $\chi^2 = 22.6$). (*B*) Percentage of kinesin beads that dissociated at the intersection from the underpass (*green triangles*) as a function of relative kinesin concentration and fit to the data (*green line*, $\chi^2 = 0.001$). (*C*) Percentage of dynein-dynactin beads that bound microtubules (*blue squares*) as a function of relative dynein-dynactin and fit to the data (*blue line*, $\chi^2 = 217$). (*D*) Percentage of dynein-dynactin beads that paused at the intersection from the underpass (*open squares*) and overpass (*solid squares*) as a function of relative dynein-dynactin concentration and fits to the data for underpass (*dashed line*, $\chi^2 = 0.016$) and overpass (*solid line*, $\chi^2 = 0.018$). For panels *A*, *C*, and *D*, the fit equation is $p = 100 \times (1 - \exp(-[\text{Motor}]/R))$, where R is the fit parameter given in the panel. For panel *B*, the fit equation is: $p = p_{\max} \times \exp(-[\text{Motor}]/R)$, where R is the fit parameter given in the panel.

engaging the intersecting microtubule are required to anchor the bead.

At the lowest dynein-dynactin densities, ~30% of placed beads bound to microtubules (Fig. 5 *C*). These beads exhibited the ability to reverse direction (Fig. 4 *B*). From single-molecule TIRF data, we know that the ability to reverse is an intrinsic property of single dynein-dynactin complexes. These data suggest that the lowest dynein-dynactin concentration corresponds to having very few or single interacting dynein-dynactin complexes per bead, and they support the earlier report (28) that more than one dynein-dynactin acting in concert seldom exhibit reversals.

DISCUSSION

Single motor complexes of kinesin and dynein-dynactin behave differently at microtubule intersections

Individual kinesin motors were more likely to pass through an intersection than single dynein-dynactin complexes, which have a more varied response (Figs. 2 and 5). In particular, single dynein-dynactin complexes were more likely to switch microtubule tracks at an intersection or reverse direction than single kinesins. The differences between kinesin and dynein likely stem from the structural differences between the motors. Because of its larger step size and flexible nature, dynein is probably able to switch at an intersection by taking a large step from the original microtubule onto the crossing microtubule. Kinesin, with its smaller stride length and straight path, is less likely to switch. It is more likely to remain on an individual protofilament and pass the intersection without influence from the intersecting microtubule. If these actions apply in the cell interior, dynein molecules could follow more diverse paths within the cell's intersecting microtubule network.

Passing through an intersection on an underpass microtubule

Single-motor fluorescence data showed a surprisingly large number of kinesin and dynein-dynactin motors that were able to pass intersections while traversing on an underpass microtubule (kinesin = 53%, dynein-dynactin = 34%, Fig. 2). In this situation, the motor could 1), traverse under the overpass microtubule if it is small enough, 2), switch twice—first to the overpass microtubule and then back to the underpass one on the opposite side, or 3), step over the overpass without interacting with the intersecting microtubule. Recent work on myosin-V in crossing actin networks suggests that this motor protein can walk over actin filaments without interacting (29).

For single kinesins, the occurrence of a single switch event is rare (4–6%), so the probability of independently switching twice is very small (probability switching twice = p(under → over) × p(over → under) = 0.04 × 0.06 = 0.002). In addition, because of the short linker between kinesin's motor head and dimerization domain, stepping over the overpass microtubule seems unlikely. Thus, we conclude that kinesin traverses the intersection by fitting under the overpass microtubule. Given kinesin's small size, this may be expected.

More surprising is the substantial probability of dynein-dynactin passing by an intersection from an underpass microtubule (0.34, Fig. 2 *B*) because dynein-dynactin is larger than kinesin. Like kinesin, dynein-dynactin could be passing under the obstruction, but it might be stepping over the overpass by its ability to take large steps (8,9). Oversteps could be double switches or noninteracting steps. The likelihood for dynein-dynactin to switch once is much higher than that for kinesin (22–24%), so the expected probability of a double switch is also expected to be higher (probability switching twice = p(under → over) × p(over → under) = 0.22 × 0.24 = 0.053). Assuming that the probability of passing from an underpass is the sum of the probabilities for double switching and squeezing under, the apparent probability that dynein-dynactin passes under is ~29% (= 34% − 5%) of underpass encounters. This estimation does not take into account the possibility of stepping over without interacting, which cannot be determined in our assay.

To gauge the influence of geometric hindrance for the motors passing under an overpass, we made a simple estimate of the relative proportion of the track microtubule circumference available to the two motors while fitting between an overpass microtubule and the glass surface (Fig. 6). This simplified model assumes that the two microtubules are in contact. Two pieces of evidence support that the microtubules are in close contact: 1), both microtubules are clearly visible in the evanescent wave of the TIRF, implying that they are within 100 nm of the surface, and 2), single dynein-dynactin complexes, which are known to take up to 32-nm steps, can switch easily (Fig. 2 *B*) from one microtubule to the other, implying that the microtubules must be within 32 nm of each other. On this assumption, the proportion of microtubule circumference, P, in the plane of the overpass, available for contact by a spherical motor of radius r is given by

$$P = \frac{2\Theta}{2\pi - \phi} = \frac{2\Theta}{\pi + \Theta} = \frac{4\sin^{-1}\{(R - r/R + r)\}}{\pi + 2\sin^{-1}\{(R - r/R + r)\}} \quad (1)$$

where Θ is the angle associated with the circumference that is accessible on each side, and $\phi = \pi - \Theta$ is the angle corresponding to the circumference that is blocked by the glass surface (Fig. 6, *inset*). The microtubules are considered to be cylinders with a diameter of 25 nm, and curvature of the overpass microtubule axis is assumed to be gradual enough that it can be considered straight.

On the initial assumption that the only impediment to passing under an overpass microtubule is physical contact with the glass or the overpass itself, the probability of passing under is proportional to the available circumference. The measured percentage of motors that pass under then leads to an effective radius. For kinesin, this percentage is 53%, which implies an effective radius of 3.8 nm (Fig. 6, *dashed marker line*). For dynein-dynactin, the percentage of motors that pass under is 29% (assuming 5% are double switches as above), giving an effective radius of 7.5 nm (Fig. 6, *solid marker line*). The radii of the kinesin and dynein motor heads are ~2 nm (30) and 5 nm (6), respectively, which are both ~1.5–2 times smaller than the corresponding effective radius. Factors that would add to the restriction of under passage are extra volume of the tail for kinesin, light chains and dynactin for dynein, binding or nonspecific interaction with the overarching microtubule, and extra volume necessary for the random component of diffusive search for the next binding site. Despite these unaccounted factors in our estimation of effective radius, the relative proportions of the two motors that pass under scale reasonably with the sizes of their heads, suggesting that the difference in passing an intersection results largely from the size differential between kinesin and dynein-dynactin.

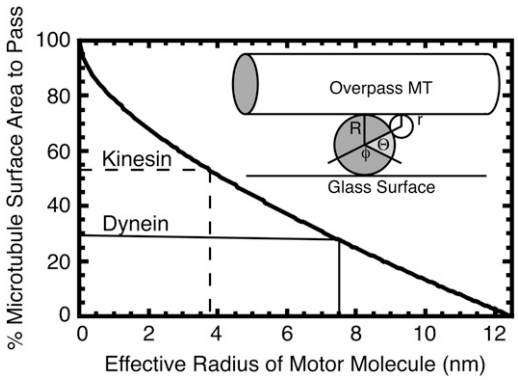

FIGURE 6 Geometric model to estimate the free microtubule circumference for kinesin or dynein to traverse an underpass without hindrance. The percentage of passable surface area is plotted as a function of effective motor radius, r, as explained in the text. When the percentage of passable surface area is 53%, then the effective motor radius is 3.8 nm, as for kinesin (*dashed marker lines*). When the percentage of passable surface area is 29%, then the effective motor radius is 7.5 nm for dynein (*solid marker lines*). (*Inset*) Schematic for the geometric model. The overpass microtubule is represented as a cylinder on top, and the underpass microtubule is seen in cross-section as a circle, both of radius R. The motor is represented as a small circle of radius r. The angle Θ corresponds to the circumference of the underpass microtubule that is accessible to the motor on each side of the microtubule. The angle ϕ corresponds to the circumference of the underpass microtubule that is permanently blocked by the glass surface.

Reversibility of the dynein-dynactin complex

The ability of individual dynein-dynactin complexes to reverse direction when encountering an obstacle along the microtubule path might facilitate navigation around such obstacles. If the microtubule intersections act as obstacles to motion in vitro, dynein-dynactin motors on underpass microtubules would then reverse more often than from overpass microtubules. Interestingly, we found no difference in the ability of single fluorescently labeled dynein-dynactin complexes to reverse from an overpass or an underpass. At very low levels of dynein-dynactin decoration, beads were able to reverse direction, as single motor complexes did (Table S1). A recent article showed that single dynein motors bound to beads can

move bidirectionally, but the addition of a second motor abolishes reverse motion (28). We observed twice as many beads reversing at intersections from underpass microtubules (22%) as from overpasses (11%, Table S1). This result implies that the microtubule might pose an obstacle to motion and cause reversals for motors bound to cargo, although to a lesser extent for single complexes.

Kinesin motors' cooperativity allows switching between microtubules at intersections

Bead cargos decorated with kinesin motors have a high probability of switching at an intersection, independent of the number of motors interacting with the microtubule, and regardless of whether approaching from an underpass or overpass (Figs. 4 *A* and 7 and Table S1). These data suggest that kinesin motors on different parts of the same bead do not maintain their attachments unremittingly but seem to coordinate dissociation to continue moving (Fig. 7). Two possible mechanisms could explain this apparent cooperativity for kinesin. First, kinesin motors on the underpass microtubule dissociate from the microtubule when they come to a blocked path. This reaction is corroborated by the observation that single kinesin motors were more likely to dissociate at an intersection when approaching from an underpass microtubule than from an overpass (Table S1). A second possible contributor to this apparent coordination is that kinesin motors might react to mechanical forces produced by motors at another location on the bead.

Often, it was clear that the motors were simultaneously bound to and exerting forces on both of the intersecting microtubules because the kinesin beads would noticeably deform the microtubules at the intersection (Fig. 3 *C*, *8.2 s* and *29.3 s*). Another recent article has reported the same phenomenon with smaller kinesin-coated beads walking on tau-decorated intersecting microtubules (31), and bending of single microtubules has been observed previously in kinesin-powered gliding assays (32). In the cell, similar microtubule-motor interactions could lead to large-scale rearrangements of the cytoskeletal microtubules because they are not bound tightly to a substrate. Such rearrangements have been seen with motor-covered melanosomes in cell fragments (33) as well as in vitro with kinesin aggregates that can arrange microtubules into asters (34,35).

After flexing of the microtubules, the outcome may depend on the number of motors bound to each microtubule—the patch with more motors would win. One would expect that kinesin-coated beads to be more likely to switch when starting on an underpass microtubule because the bead would interact with both microtubules easily in that situation. This is exactly what we observed: 66% of beads switch from an underpass to an overpass. Fewer (33%) kinesin-decorated beads switched from the overpass to the underpass microtubule (Fig. 4 *A*). The increased probability for switching from underpass to overpass is likely caused by two factors: 1), increased dissociation of motors on the underpass because the overpass microtubule acts as an obstacle, and 2), increased chances of interacting with both microtubules simultaneously because the overpass blocks the path of forward motion.

Dynein motors act as cargo tethers at high motor concentration

At all levels of dynein-dynactin decoration, bead cargos are most likely to pause at an intersection, whether approaching from an overpass or an underpass, and the percentage of pausing increases to ~100% at the highest motor concentration (Figs. 4 *B*, 5 *D*, and 7). Unlike kinesin, the dynein motors on various parts of the same bead do not appear to cooperate to facilitate switching between tracks, but rather, they stay attached, leading to pausing. It is interesting that dynein motors do not appear to struggle against each other when moving beads along single microtubules, but when the direction of motion is altered, such as at an intersection, the motors become moored at the intersection.

As mentioned earlier, tethering by dynein-dynactin intersections depends on relative dynein-dynactin concentration because $p_{\text{pause}} = 100 \times (1 - \exp(-[\text{Dyn}]/R_{\text{d,2}}))$ with a similar fitted dilution, $R_{\text{d,2}}$, to that required for beads to bind and move along single microtubules, $R_{\text{d,1}}$ (Fig. 5, *C* and *D*). These relationships imply that one or a few complexes are sufficient to mediate pausing. One dynein-dynactin complex could attach to both microtubules via the microtubule binding sites on dynein and dynactin. Another possibility is that individual heads of dynein can span across and bind simultaneously to two microtubules. The kinetics of mammalian dynein suggest that the two heads are not well coordinated, so each head might bind tightly to a different microtubule. Kinesin, on the other hand, has a synchronized stepping mechanism such that both heads do not simultaneously bind tightly during normal stepping; this intramolecular signaling would make tethering by a single kinesin molecule unlikely. In addition, single molecules of dynein-dynactin are observed to switch often in TIRF assays, whereas single kinesins rarely do, supporting the idea that a single dynein-dynactin can span the microtubule intersection.

There is an intriguing inverse correlation between dynein-dynactin pausing and reversing. As we and others have noted earlier (10,28,36), the ability for dynein-dynactin to move toward the plus end (opposite to its predominant direction) is an intrinsic property of the single motor complex. At the lowest dynein-dynactin density, beads exhibited reversals (11–22% of the trials) and paused in about half the cases from an underpass (Fig. 4 *B*). At the next highest density (loading dilution, 0.1), beads stopped reversing altogether, which implies that more than one motor was operating. Interestingly, this was the same motor density at which pausing increased dramatically to 92% for beads reaching an intersection from an underpass. These results suggest that only a few motors, possibly only two per microtubule, suppress

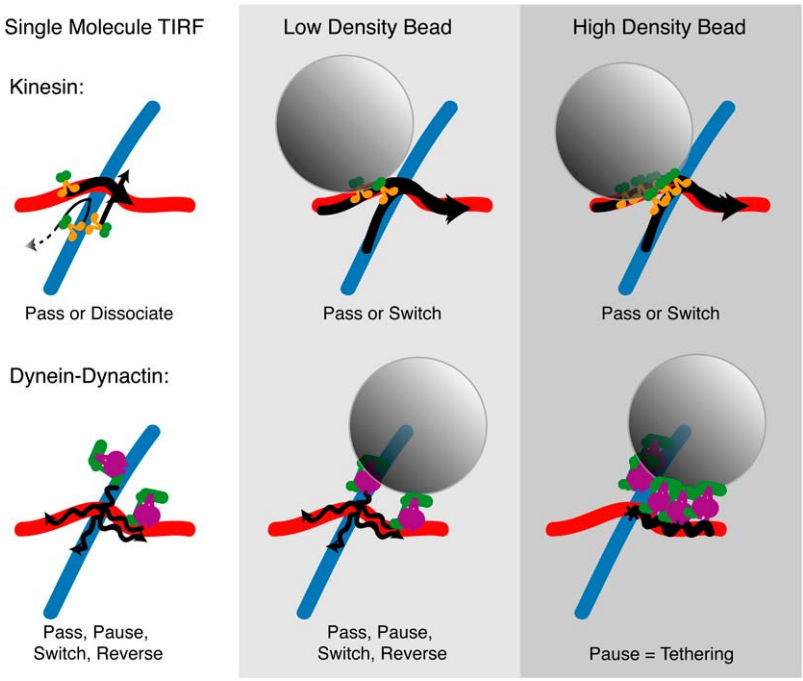

FIGURE 7 Cartoon depiction of the results of single-molecule TIRF and low-density and high-density motor decoration on motility in vitro. Single molecules of kinesin mostly pass and dissociate, whereas single dynein-dynactin complexes can pass, pause, dissociate, switch, and reverse direction (*left column*). Adding the complexity of a bead cargo with very few motors (*middle column*) allows kinesin to pass but also to switch frequently. Dynein-dynactin bound to beads at low density allows similar actions, with less passing on an underpass and more pausing, but also some reversing and switching (*middle column*). Increasing the density of bound kinesin does not significantly change the actions of cargo at intersections, but increasing the density of dynein-dynactin causes all cargo to become tethered at intersections (*right column*). Wavy lines denote lateral wobbling of the dynein-dynactin bead cargo.

reversals, maintain attachment with the track microtubule, and promote long-lived association with the intersecting microtubule.

Dynein lateral displacements increase tethering at intersections from overpass microtubules

We found that kinesin beads mostly passed intersections when traveling on the overpass microtubule (69%), but dynein-dynactin beads rarely passed at intersections (0–33%). The difference between kinesin and dynein-dynactin is most likely a result of the ability of dynein-dynactin to diffuse or move laterally across the surface of the microtubule. These attributes of dynein are clearly defined and analyzed in previous work (9,36). Such lateral excursions increase the chance of interactions with the underpass microtubule (Fig. 7). Kinesins, which are known to walk along a single protofilament, are less likely to interact with the underpass microtubule.

Biological implications of dynein-dynactin tethering

The ability of dynein to act as an anchor for cargos may be fundamental to its cellular function of maintaining and rearranging cellular architecture during interphase, mitosis, and cytokinesis (37–39). In our in vitro system, there are no chemical or posttranslational regulators of dynein, but our data clearly show a qualitative change in dynein action that depends on the number of dynein motors involved. With one motor, dynein is flexible and able to perform a variety of actions at an intersection, but with many motors, dynein anchors bead cargos at microtubule intersections. Changing the number of motors bound to a cargo or their relative activity may provide a simple mechanism for controlling the relative numbers of motile versus tethered cargos in the cell. In addition, the sensitivity to motor number implies that pausing can be initiated with relatively few motors. This change from moving to pausing could be important to arranging cargos at specific locations in the cell.

In particular, the Golgi apparatus is tethered at the microtubule-organizing center near the nucleus by dynein-dynactin. When dynein-dynactin is disrupted, Golgi vesicles are dispersed throughout the cell by kinesin (40). This observation suggests that kinesin and dynein-dynactin are both bound to the Golgi, but the tethering activity of dynein is dominant. Dynein also tethers microtubule ends to the cell cortex (41) and may secure other biological cargos, such as mitochondria and RNA granules, along microtubule tracks (42,43). Based on our in vitro observations, we predict that the in vivo switch from motile to tethered cargo may be regulated by motor number as well as motor activity. Studies to test this model are now in progress.

SUPPLEMENTARY MATERIAL

To view all of the supplemental files associated with this article, www.biophysj.org.

Thank you to Andrew Loh, Rama Kudaravalli, Huy Pham, Wiley Zhou, and Mariko Tokito.

This work was supported by the National Institutes of Health (NIH) project program grant P01-AR-051174 to the Pennsylvania Muscle Institute, National Science Foundation grant NSEC DMR04-25780 to the Penn Nano/Bio Interface Center, and by NIH GM068591 to E.L.F.H. J.L.R. was supported by an NIH National Research Service Award grant 1F32GM075754-01. The authors have no competing interests.

REFERENCES

1. Vale, R. D. 2003. The molecular motor toolbox for intracellular transport. *Cell.* 112:467–480.
2. Svoboda, K., C. F. Schmidt, B. J. Schnapp, and S. M. Block. 1993. Direct observation of kinesin stepping by optical trapping interferometry. *Nature.* 365:721–727.
3. Cai, D., A. D. Hoppe, J. A. Swanson, and K. J. Verhey. 2007. Kinesin-1 structural organization and conformational changes revealed by FRET stoichiometry in live cells. *J. Cell Biol.* 176:51–63.
4. Kon, T., M. Nishiura, R. Ohkura, Y. Y. Toyoshima, and K. Sutoh. 2004. Distinct functions of nucleotide-binding/hydrolysis sites in the four AAA modules of cytoplasmic dynein. *Biochemistry.* 43:11266–11274.
5. Burgess, S. A., M. L. Walker, H. Sakakibara, P. J. Knight, and K. Oiwa. 2003. Dynein structure and power stroke. *Nature.* 421:715–718.
6. Meng, X., M. Samsó, and M. P. Koonce. 2006. A flexible linkage between the dynein motor and its cargo. *J. Mol. Biol.* 357:701–706.
7. King, S. J., and T. A. Schroer. 2000. Dynactin increases the processivity of the cytoplasmic dynein motor. *Nat. Cell Biol.* 2:20–24.
8. Mallik, R., B. C. Carter, S. A. Lex, S. J. King, and S. P. Gross. 2004. Cytoplasmic dynein functions as a gear in response to load. *Nature.* 427:649–652.
9. Reck-Peterson, S. L., A. Yildiz, A. P. Carter, A. Gennerich, N. Zhang, and R. D. Vale. 2006. Single-molecule analysis of dynein processivity and stepping behavior. *Cell.* 126:335–348.
10. Ross, J. L., K. Wallace, H. Shuman, Y. E. Goldman, and E. L. Holzbaur. 2006. Processive bidirectional motion of dynein-dynactin complexes in vitro. *Nat. Cell Biol.* 8:562–570.
11. Wang, Z., and M. P. Sheetz. 2000. The C-terminus of tubulin increases cytoplasmic dynein and kinesin processivity. *Biophys. J.* 78:1955–1964.
12. Karki, S., and E. L. Holzbaur. 1995. Affinity chromatography demonstrates a direct binding between cytoplasmic dynein and the dynactin complex. *J. Biol. Chem.* 270:28806–28811.
13. Schroer, T. A. 2004. Dynactin. *Annu. Rev. Cell Dev. Biol.* 20:759–779.
14. Yildiz, A., M. Tomishige, R. D. Vale, and P. R. Selvin. 2004. Kinesin walks hand-over-hand. *Science.* 303:676–678.
15. Fuchs, E., and I. Karakesisoglou. 2001. Bridging cytoskeletal intersections. *Genes Dev.* 15:1–14.
16. Helfand, B. T., A. Mikami, R. B. Vallee, and R. D. Goldman. 2002. A requirement for cytoplasmic dynein and dynactin in intermediate filament network assembly and organization. *J. Cell Biol.* 157:795–806.
17. Rogers, S. L., and V. I. Gelfand. 1998. Myosin cooperates with microtubule motors during organelle transport in melanophores. *Curr. Biol.* 8:161–164.
18. Kapoor, T. M., M. A. Lampson, P. Hergert, L. Cameron, D. Cimini, E. D. Salmon, B. F. McEwen, and A. Khodjakov. 2006. Chromosomes can congress to the metaphase plate before biorientation. *Science.* 311: 388–391.
19. Reilein, A., S. Yamada, and W. J. Nelson. 2005. Self-organization of an acentrosomal microtubule network at the basal cortex of polarized epithelial cells. *J. Cell Biol.* 171:845–855.
20. Pierce, D. W., and R. D. Vale. 1998. Assaying processive movement of kinesin by fluorescence microscopy. *Methods Enzymol.* 298:154–171.
21. Hancock, W. O., and J. Howard. 1999. Kinesin's processivity results from mechanical and chemical coordination between the ATP hydrolysis cycles of the two motor domains. *Proc. Natl. Acad. Sci. USA.* 96:13147–13152.
22. Vale, R. D., T. Funatsu, D. W. Pierce, L. Romberg, Y. Harada, and T. Yanagida. 1996. Direct observation of single kinesin molecules moving along microtubules. *Nature.* 380:451–453.
23. Valentine, M. T., P. M. Fordyce, T. C. Krzysiak, S. P. Gilbert, and S. M. Block. 2006. Individual dimers of the mitotic kinesin motor Eg5 step processively and support substantial loads in vitro. *Nat. Cell Biol.* 8:470–476.
24. Kaseda, K., H. Higuchi, and K. Hirose. 2003. Alternate fast and slow stepping of a heterodimeric kinesin molecule. *Nat. Cell Biol.* 5:1079–1082.
25. Takagi, Y., E. E. Homsher, Y. E. Goldman, and H. Shuman. 2006. Force generation in single conventional actomyosin complexes under high dynamic load. *Biophys. J.* 90:1295–1307.
26. Klumpp, S., and R. Lipowsky. 2005. Cooperative cargo transport by several molecular motors. *Proc. Natl. Acad. Sci. USA.* 102:17284–17289.
27. Svoboda, K., and S. M. Block. 1994. Force and velocity measured for single kinesin molecules. *Cell.* 77:773–784.
28. Mallik, R., D. Petrov, S. A. Lex, S. J. King, and S. P. Gross. 2005. Building complexity: an in vitro study of cytoplasmic dynein with in vivo implications. *Curr. Biol.* 15:2075–2085.
29. Ali, M. Y., E. B. Krementsova, G. G. Kennedy, R. Mahaffy, T. D. Pollard, K. M. Trybus, and D. M. Warshaw. 2007. Myosin Va maneuvers through actin intersections and diffuses along microtubules. *Proc. Natl. Acad. Sci. USA.* 104:4332–4336.
30. Kozielski, F., S. Sack, A. Marx, M. Thormählen, E. Schönbrunn, V. Biou, A. Thompson, E. M. Mandelkow, and E. Mandelkow. 1997. The crystal structure of dimeric kinesin and implications for microtubule-dependent motility. *Cell.* 91:985–994.
31. Vershinin, M., B. C. Carter, D. S. Razafsky, S. J. King, and S. P. Gross. 2007. Multiple-motor based transport and its regulation by Tau. *Proc. Natl. Acad. Sci. USA.* 104:87–92.
32. Vale, R. D., C. M. Coppin, F. Malik, F. J. Kull, and R. A. Milligan. 1994. Tubulin GTP hydrolysis influences the structure, mechanical properties, and kinesin-driven transport of microtubules. *J. Biol. Chem.* 269:23769–23775.
33. Vorobjev, I., V. Malikov, and V. Rodionov. 2001. Self-organization of a radial microtubule array by dynein-dependent nucleation of microtubules. *Proc. Natl. Acad. Sci. USA.* 98:10160–10165.
34. Nédélec, F. J., T. Surrey, A. C. Maggs, and S. Leibler. 1997. Self-organization of microtubules and motors. *Nature.* 389:305–308.
35. Surrey, T., F. Nedelec, S. Leibler, and E. Karsenti. 2001. Physical properties determining self-organization of motors and microtubules. *Science.* 292:1167–1171.
36. Wang, Z., S. Khan, and M. P. Sheetz. 1995. Single cytoplasmic dynein molecule movements: characterization and comparison with kinesin. *Biophys. J.* 69:2011–2023.
37. Burkhardt, J. K., C. J. Echeverri, T. Nilsson, and R. B. Vallee. 1997. Overexpression of the dynamitin (p50) subunit of the dynactin complex disrupts dynein-dependent maintenance of membrane organelle distribution. *J. Cell Biol.* 139:469–484.
38. Gaglio, T., A. Saredi, J. B. Bingham, M. J. Hasbani, S. R. Gill, T. A. Schroer, and D. A. Compton. 1996. Opposing motor activities are required for the organization of the mammalian mitotic spindle pole. *J. Cell Biol.* 135:399–414.
39. Karki, S., B. LaMonte, and E. L. Holzbaur. 1998. Characterization of the p22 subunit of dynactin reveals the localization of cytoplasmic dynein and dynactin to the midbody of dividing cells. *J. Cell Biol.* 142:1023–1034.
40. Caviston, J. P., J. L. Ross, S. M. Antony, M. Tokito, and E. L. Holzbaur. 2007. Huntingtin facilitates dynein/dynactin-mediated vesicle transport. *Proc. Natl. Acad. Sci. USA.* 104:10045–10050.
41. Ligon, L. A., S. Karki, M. Tokito, and E. L. Holzbaur. 2001. Dynein binds to β-catenin and may tether microtubules at adherens junctions. *Nat. Cell Biol.* 3:913–917.
42. Bullock, S. L., A. Nicol, S. P. Gross, and D. Zicha. 2006. Guidance of bidirectional motor complexes by mRNA cargoes through control of dynein number and activity. *Curr. Biol.* 16:1447–1452.
43. Varadi, A., L. I. Johnson-Cadwell, V. Cirulli, Y. Yoon, V. J. Allan, and G. A. Rutter. 2004. Cytoplasmic dynein regulates the subcellular distribution of mitochondria by controlling the recruitment of the fission factor dynamin-related protein-1. *J. Cell Sci.* 117:4389–4400.